JOURNAL OF APPLIED ELECTROCHEMISTRY **28** (1998) 1121–1125

Reduction of nitrogen monoxide to nitrogen at gas diffusion electrodes with noble metal catalysts

M. SHIBATA, K. MURASE, N. FURUYA

Department of Applied Chemistry, Faculty of Engineering, Yamanashi University, 4-3-11 Takeda, Kofu 400, Japan

Received 27 October 1997; accepted in revised form 9 February 1998

The electrochemical reduction of NO in alkaline solutions was investigated at gas diffusion electrodes with various metal (Ru, Rh, lr, Pd and Pt) catalysts at various NO flow rates. Reduction currents are observed at potentials more negative than 0.95 V, which increase with the decrease in potential and also with increasing gas flow rate. The faradaic efficiencies of N_2O formation decrease with decreasing NO flow rate and with decrease in potential. The faradaic efficiencies of N_2 formation increase with decreasing flow rate and with decrease in potential. The reduction of NO to N_2 at a flow rate of 5 ml min^{-1} occurs selectively at potentials more negative than 0.1 V; the faradaic efficiency of N_2 formation is approximately 95% at Pd catalysts.

Electricity production and NO decomposition can be carried out simultaneously using an H_2–NO fuel cell reactor. The faradaic efficiency of N_2 formation at a flow rate of 5 ml min^{-1} is approximately 80% at a cell voltage of 0.25 V.

Keywords: *fuel cell*, *gas diffusion electrodes*, *noble metal catalysts*, *NO reduction*

1. Introduction

The evolution of nitrogen oxides (i.e., nitrogen monoxide (NO) and nitrogen dioxide (NO_2) being air pollutants) is exerting an influence upon the human body and causes serious problems such as acid rain and photochemical smog. One of the solutions to this problem is to chemically decompose NO to N_2. Many papers have been published on NO removal in the gas phase [1–6]. Moreover, NO adsorption has been investigated on noble metal catalysts having a well-defined surface [7–9]. However, the electrochemical process for the reduction of NO to N_2 has been less well studied, although there are several articles on NO reduction aimed at the formation of hydroxylamine in acid solutions [10, 11]. It was reported that the main products of NO reduction in acid solutions are ammonia, hydroxylamine, N_2O etc. [10–14].

For NO removal, NO is reduced to N_2 mostly via N_2O. Investigating N_2O reduction at the (1 0 0), (1 1 0) and (1 1 1) faces of a Pt single crystal in acid solutions, Ebart *et al*., [15] reported that N_2O can be reduced to N_2 in the region of hydrogen adsorption. The rate of N_2O reduction to N_2 in acid solutions is, however, much lower than in alkaline solutions [16–18]. Consequently, N_2 cannot be formed during NO reduction in acid solutions.

In alkaline solutions N_2O is easily reduced to N_2 at noble metal catalysts [18, 19]. N_2O formed during NO reduction will be reduced to N_2 in alkaline solutions. Therefore, we expected that NO reduction to N_2 can easily take place at the catalysts in alkaline solutions. We have investigated a fuel cell reaction (H_2–N_2O) at a gas diffusion electrode with various metal catalysts [17, 18]. It became clear that N_2O can be decomposed to N_2 (faradaic efficiency 100%) and the H_2–N_2O fuel cells can be operated with the use of 1 M KOH solution as electrolyte.

In this work, the electrochemical reduction of NO to N_2 and the fuel cell reaction (H_2–NO) were investigated at gas diffusion electrodes with various noble metal (Ru, Rh, Ir, Pd and Pt) catalysts in alkaline solutions.

2. Experimental details

2.1. *Electrodes*

A gas diffusion electrode (40 mm in diameter and apparent working area of 12.6 cm^2) was used as a working electrode. The gas diffusion electrode [20] consisted of a gas diffusion layer and a reaction layer composed of a mixture of a hydrophilic portion and a hydrophobic portion. The hydrophilic portion was made of powder P1 which blends a hydrophilic carbon black and polytetrafluoroethylene. The hydrophobic portion was made of the powder P2 that blends a hydrophobic carbon black and polytetrafluoroethylene. The gas diffusion layer made of powder P2 has many hydrophobic micropores and the dual function of (i) supplying NO gas to the reaction layer and (ii) preventing the infiltration of electrolyte. The reaction layer, the gas diffusion layer and a copper mesh for electrical contact were pressed under the experimental condi-

0021-891X

tion of 653 K and 6000 N cm^{-2}. Chloroplatinic acid hexahydrate, palladium(II) chloride, iridium(III) chloride, ruthenium(III) chloride, rhodium chloride trihydrate, copper chloride, silver nitrate and chloroauric acid solutions of 3.6×10^{-5} mol were applied to the reaction layer at the gas diffusion electrode, dried and oxidized for 1 h at 473 K. The metal oxides formed in the reaction layer were reduced by hydrogen gas for 2 h at 473 K.

A Pt-loaded gas diffusion electrode provided with hydrogen gas and an SCE were used as an auxiliary electrode and a reference electrode, respectively. All the electrode potentials in this paper refer to the RHE.

2.2. *Cell, electrolyte and electrolysis*

The electrolysis cell, as shown in Fig. 1, consists of the two gas diffusion electrodes 5 mm apart. The supporting electrolyte solutions examined contained 1 mol dm^{-3} (M) KOH. Controlled potential electrolysis was carried out at a gas diffusion electrode under ambient pressure and temperature, 298 K, while NO was supplied at a constant flow rate (5, 10, 15 and 30 ml min^{-1}) from the backsides of the cathode. The electrolysis was conducted for 10 min at each potential.

2.3. *Analysis of products*

During electrolysis, H_2, N_2 and N_2O in the gas phase were analysed by gas chromatography (Hitachi 263-30, Japan) on Molecular Sieve 5A and 13XS column (GL science, Tokyo) at 403K. After electrolysis for 10 min, NO_2^- and NO_3^- in the electrolyte were measured with a liquid chromatograph (Shimadzu, LC-6A), and then hydroxylamine, hydrazine and ammonia were determined by a spectrophotometer (Hitachi, U-2000).

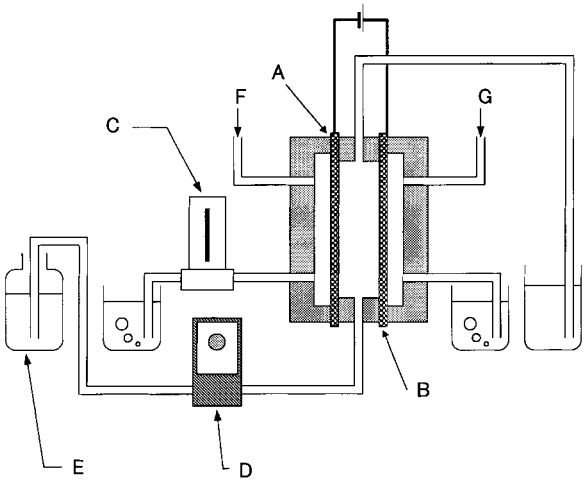

Fig. 1. Schematic diagram of the electrolysis equipment. A: cathode with various metal catalysts; B: anode with Pt catalysts; C: flow meter; D: pump; E: electrolyte (1 M KOH); F: N_2O gas inlet; G: H_2 gas inlet.

3. Results and discussion

3.1. *Rate of NO reduction*

Figure 2 shows the polarization curves for a gas diffusion electrode with Pd catalysts in 1 M KOH. Reduction currents are observed at potentials more negative than 0.95 V and increase with decrease in potential. At 0.2 V, the currents at flow rates of 30, 15, 10 and 5 ml min^{-1} are −0.114, −0.099, −0.078 and −0.046 A cm^{-2}, respectively. The reduction currents decrease with decreasing gas flow rate.

Figure 3 shows the polarization curves for a gas diffusion electrode with Pt catalysts in 1 M KOH. Reduction currents are observed at potentials more negative than 1 V and increase with the decrease in potential. At 0.2 V, the currents at 30, 15, 10 and 5 ml min^{-1} are −0.113, −0.073, −0.062 and −0.047 A cm^{-2}, respectively. The reduction currents decrease with decreasing flow rate.

Figure 4 shows the polarization curves for gas diffusion electrodes with Rh, Ir and Ru catalysts in 1 M KOH. Reduction currents are observed at potentials more negative than 1 V and increase with the decrease in potential.

At 0.2 V, the currents at Rh, Ir and Ru catalysts are −0.045, −0.042, and −0.022 A cm^{-2}, respectively. The activity for NO reduction increases in the order

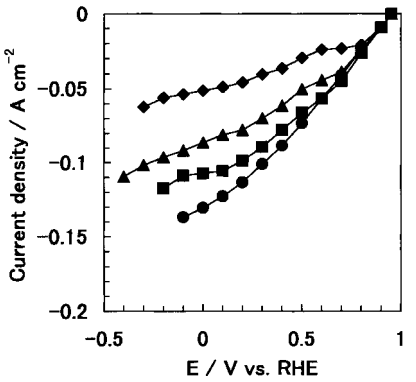

Fig. 2. Polarization curves obtained at different NO gas flow rate at a gas diffusion electrode with Pd catalysts in 1 M KOH. Key: (●) 30, (■) 15, (▲) 10, and (◆) 5 ml min^{-1}.

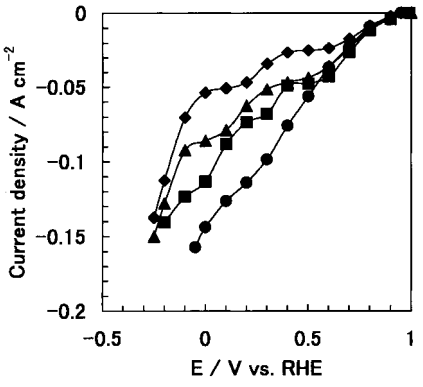

Fig. 3. Polarization curves obtained at different NO gas glow rate at a gas diffusion electrode with Pt catalysts in 1 M KOH. Key: (●) 30, (■) 15, (▲) 10, and (◆) 5 ml min^{-1}.

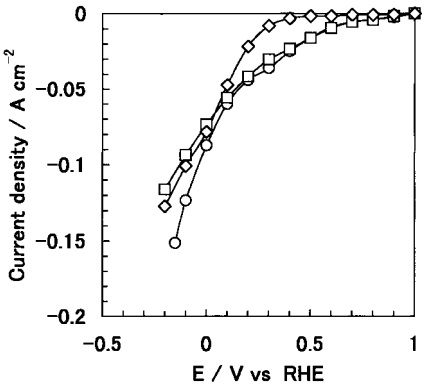

Fig. 4. Polarization curves obtained at the flow rate of 30 ml min^{-1} at gas diffusion electrodes with metal catalysts in 1 M KOH. Key: (○) Rh catalysts, (□) Ir catalysts, and (◇) Ru catalysts.

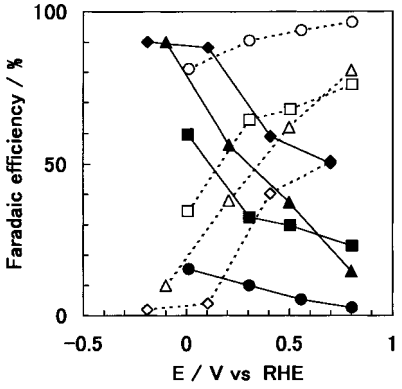

Fig. 6. Faradaic efficiencies obtained at different NO gas flow rate as a function of potential at a gas diffusion electrode with Pt catalysts in 1 M KOH Solution. Formation of N_2 (—) and N_2O (- - - -). Key: (●, ○) 30, (■, □) 15, (▲, △) 10, (◆, ◇) 5 ml min^{-1}.

of the catalysts Pd ≥ Pt ≫ Rh = Ir > Ru at potentials more positive than 0.2 V.

3.2. *Reduction of NO to N_2O and N_2*

Faradaic efficiencies for products of NO reduction at Pd catalysts were plotted against electrode potential in Fig. 5. Faradaic efficiencies of N_2O formation are approximately 100% at a flow rate of 30 ml min^{-1}, while N_2 formation takes place only to a small extent at potentials more negative than 0.3 V. The faradaic efficiencies of N_2O formation decrease with decreasing NO flow rate and with decrease in potential. However, the faradaic efficiencies of N_2 formation increase with decreasing NO flow rate and with decrease in potential. The reduction of NO to N_2 at 5 ml min^{-1} occurs selectively at potentials more negative than 0.1 V; the faradaic efficiency is approximately 95%. Hydrogen evolution cannot take place at potentials more positive than −0.2 V. Trace amounts of hydroxylamine, hydrazine and ammonia were detected in the electrolyte after electrolysis. NO conversion (flow rate 5 ml min^{-1}, potential 0 V) at the Pd catalysts is approximately 50%.

Faradaic efficiencies of the products of NO reduction at the Pt catalysts were plotted against electrode potential in Fig. 6. Faradaic efficiencies of N_2O formation increase with decreasing overpotential, while faradaic efficiencies of N_2 formation increase with increasing overpotential. The faradaic efficiencies of N_2O formation decrease with decreasing NO flow rate. However, the faradaic efficiencies of N_2 formation increase with decreasing NO flow rate. The reduction of NO to N_2 at 5 ml min^{-1} occurs selectively at potentials more negative than 0.1 V; the faradaic efficiency is approximately 90%. The faradaic efficiency of ammonia formation is approximately 5% at 0 V and decreases with decreasing overpotential. Trace amounts of hydroxylamine and hydrazine were detected in the electrolyte after electrolysis. Hydrogen evolution cannot take place at potentials more positive than −0.2 V. NO conversion (flow rate 5 ml min^{-1}, potential = 0 V) at Pt catalysts is approximately 60% .

Faradaic efficiencies of the products of NO reduction at the Rh catalysts were plotted against the electrode potential in Fig. 7. The faradaic efficiency of N_2O formation at 0.5 V is approximately 85% at 30 ml min^{-1}, while the faradaic efficiency of N_2 formation is approximately 10%. The faradaic efficiencies of N_2O formation decrease with decreasing NO flow rate and with the decrease in potential. However, the faradaic efficiencies of N_2 formation increase with

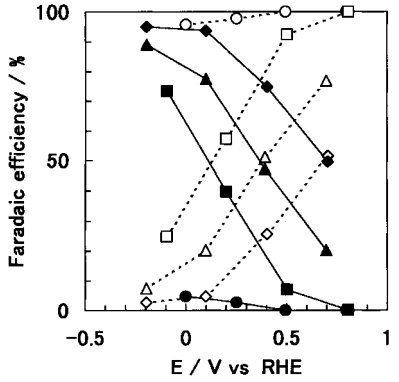

Fig. 5. Faradaic efficiencies obtained at different NO gas flow rate as a function of potential at a gas diffusion electrode with Pd catalysts in 1 M KOH Solution. Formation of N_2 (—) and N_2O (- - - -). Key: (●, ○) 30, (■, □) 15, (▲, △) 10, and (◆, ◇) 5 ml min^{-1}.

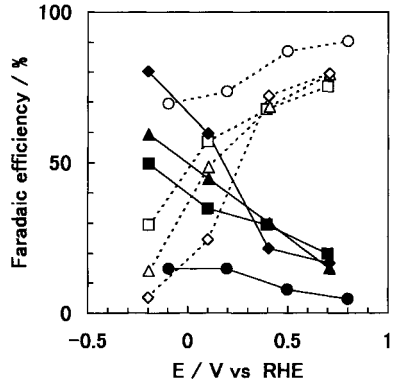

Fig. 7. Faradaic efficiencies obtained at different NO gas flow rate as a function of potential at a gas diffusion electrode with Rh catalysts in 1M KOH Solution. Formation of N_2 (—) and N_2O (- - - -). Key: (●, ○) 30, (■, □) 15, (▲, △) 10, and (◆, ◇) 5 ml min^{-1}.

decreasing NO flow rate and with the decrease in potential. The reduction of NO to N_2 at 5 ml min^{-1} occurs selectively at 0 V; the faradaic efficiency is approximately 65% . Irrespective of NO flow rate, the faradaic efficiency of ammonia formation is approximately 15% at 0 V and decreases with decreasing overpotential. Trace amounts of hydroxylamine and hydrazine were detected in the electrolyte after electrolysis. Correlation between the faradaic efficiencies of the products of NO reduction and the potentials at Ir and Ru catalysts is similar to that at Rh catalysts.

3.3. *Mechanism of NO reduction at gas diffusion electrodes with catalysts*

The following mechanism of NO reduction at a Pt electrode in acid solutions was proposed [13, 14];

$$NO + H^+ \rightarrow NOH^+ \quad (1)$$

$$NOH^+ + e^- \rightarrow NOH \quad (2)$$

$$NOH + H^+ \rightarrow HNOH^+ \quad (3)$$

$$HNOH^+ + H^+ + 2e^- \rightarrow NH_2OH \quad (4)$$

$$NH_2OH + H^+ \rightarrow NH_3OH^+ \quad (5)$$

$$NH_3OH^+ + H^+ + 2e^- \rightarrow NH_3 + H_2O \quad (6)$$

$$2NOH \rightarrow N_2O_2H_2 \rightarrow N_2O + H_2O \quad (7)$$

Ammonia, hydroxylamine and N_2O were found during NO reduction in acid solutions, while N_2 formation hardly occurred [10–13]. The rate of N_2O reduction to N_2 in acid solutions is, therefore, remarkably lower than that of the formation of NH_2OH and NH_3.

NO reduction in alkaline solutions can be described as follows:

$$NO + H_2O + e^- \rightarrow NOH + OH^- \quad (8)$$

$$NOH + 2H_2O + 2e^- \rightarrow NH_2OH + 2OH^- \quad (9)$$

$$NH_2OH + H_2O + 2e^- \rightarrow NH_3 + 2OH^- \quad (10)$$

$$2NOH \rightarrow N_2O_2H_2 \rightarrow N_2O + H_2O \quad (11)$$

$$N_2O + H_2O + 2e^- \rightarrow N_2 + 2OH^- \quad (12)$$

Because hydroxylamine and ammonia are only formed to a small extent on NO reduction as previously described, Equations 9 and 10 hardly occur in alkaline solutions. Besides N_2O, large amounts of N_2 are formed in alkaline solutions as shown in Figs 5–7. Therefore, the main reactions of NO reduction are the sucessive Equations 8, 11 and 12. When the current density increases with increasing overpotential, NO conversion is higher, and the faradaic efficiency of N_2 formation becomes large (cf. Figs 5–7). Because the partial pressure of N_2O formed is high at the high NO conversion, Equation 12 occurs with ease [17, 18].

Johnson and Sawyer reported that the maximum current for N_2O reduction on a Pt electrode in alkaline solutions gradually decreases during cycling between 0.55 and 0.05 V using cyclic voltammetry [16]. The following mechanism of N_2O reduction at a Pt electrode was proposed [16]:

$$Pt + 2OH^- \rightarrow PtO + H_2O + 2e^- \quad (13)$$

$$PtO + H_2O + 2e^- \rightarrow Pt* + 2OH^- \quad (14)$$

$$Pt* + N_2O \rightarrow Pt - N_2O \quad (15)$$

$$Pt - N_2O + H_2O + 2e^- \rightarrow Pt + N_2 + 2OH^- \quad (16)$$

The overall reaction of Equations 13–16 is identical with Equation 12. It was mentioned that N_2O reduction takes place at a clean Pt surface, which is poisoned within a short time [16]. The poisoned Pt electrode can be refreshed by Reactions 13 and 14.

In contrast, N_2O reduction at gas diffusion electrodes having Pt catalysts without refreshing the surface was steadily observed for at least 30 min. This implies that Reaction 16 occurs at the catalysts supported at a gas diffusion electrode without refreshing the surface (cf. Reactions 13 and 14). It may be expected that the metal catalysts loaded on carbon black are hardly poisoned.

The current decay of NO reduction was not found at gas diffusion electrodes with the metal catalysts. It seems that the metal catalysts loaded on carbon black are hardly poisoned during the reduction of NO to N_2O and of N_2O to N_2.

3.4. *H_2–NO fuel cells*

A fuel cell reactor is similar to the electrolysis equipment as shown in Fig. 1, but without a power source. Moreover, the reactor consists of two gas diffusion electrodes 2 mm apart. The correlation between the cell voltage of the H_2–NO fuel cell and current density was examined under ambient pressure and temperature. The products of NO reduction were also analysed at the cathode.

Figure 8 shows a cell voltage (without IR compensation) of the H_2–NO fuel cell consisting of a cathode with Pd catalysts. The current densities at a cell voltage of 0.25 V at flow rates of 30, 15, 10 and 5 ml min^{-1} are 0.087, 0.078, 0.064 and 0.038 A cm^{-2}, respectively. Moreover, the faradaic efficiencies of N_2 formation under this condition are approximately 1, 20, 50 and 80%, respectively. The formation of N_2O

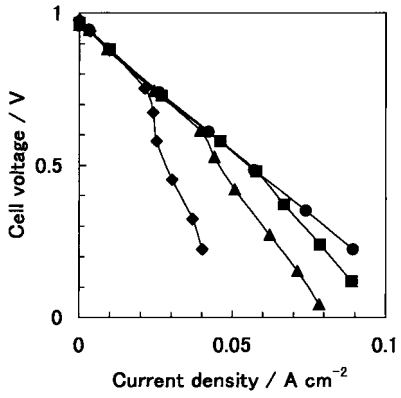

Fig. 8. Cell voltage obtained at different NO gas flow rate as a function of current density at a gas diffusion electrode with Pd catalysts using 1 M KOH solution. Key: (●) 30, (■) 15, (▲) 10, and (◆) 5 ml min^{-1}.

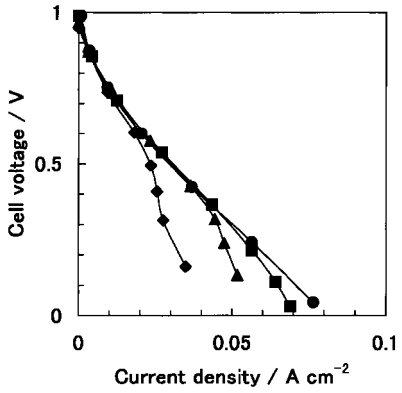

Fig. 9. Cell voltage obtained at different NO gas flow rate as a function of current density at a gas diffusion electrode with Pt catalysts using 1 M KOH solution. Key: (●) 30, (■) 15, (▲) 10, and (◆) 5 ml min^{-1}.

occurs selectively at 30 ml min^{-1}. The yield of N_2 based on moles of NO is approximately 25% at 5 ml min^{-1}. NO is completely reduced to N_2 at a flow rate of less than 10 ml min^{-1}, when two fuel cells were connected in series.

Figure 9 shows a cell voltage (without IR compensation) of the H_2–NO fuel cell consisting of a cathode with Pt catalysts. The current densities at 0.25 V at flow rates of 30, 15, 10 and 5 ml min^{-1} are 0.057, 0.054, 0.047 and 0.031 A cm^{-2}, respectively. The faradaic efficiency of N_2 formation under this condition increases with decreasing NO flow rate. The yield of N_2 based on the moles of reactant at the Pt catalysts is less than that at the Pd catalysts.

The standard reduction potentials of Equations 17, 18, 19 and 20 are +1.68, 1.59, 0.38 and 0.73V vs SHE, respectively.

$$2\,NO + 4\,H^+ + 4\,e^- \rightarrow N_2 + 2\,H_2O \quad (17)$$

$$2\,NO + 2\,H^+ + 2\,e^- \rightarrow N_2O + H_2O \quad (18)$$

$$2\,NO + 6\,H^+ + 6\,e^- \rightarrow 2\,NH_2OH \quad (19)$$

$$2\,NO + 10\,H^+ + 10\,e^- \rightarrow 2\,NH_3 + 2\,H_2O \quad (20)$$

NO can react spontaneously with hydrogen to form N_2, N_2O, NH_2OH and NH_3. Because the cell voltage of a fuel cell was approximately 0.5 V at 0.05 A cm^{-2}, as shown in Fig. 8, Equations 19 and 20 cannot occur in a fuel cell. Therefore, NO should be reduced to N_2 and N_2O by hydrogen in an H_2–NO fuel cell. Because the main products of NO reduction in an alkaline solution are N_2 and N_2O, as shown in Section 3.2, the electrochemical reaction is as follows:

The cathode reaction is

$$2\,NO + 2\,H_2O + 4\,e^- \rightarrow N_2 + 4\,OH^- \quad (21)$$

and/or

$$4\,NO + 2\,H_2O + 4\,e^- \rightarrow 2\,N_2O + 4\,OH^- \quad (22)$$

the anode reaction is

$$2\,H_2 + 4\,OH^- \rightarrow 2\,H_2O + 4\,e^- \quad (23)$$

the overall reaction is therefore

$$2\,NO + 2\,H_2 \rightarrow N_2 + 2\,H_2O \quad (24)$$

and/or

$$4\,NO + 2\,H_2 \rightarrow 2\,N_2O + 2\,H_2O \quad (25)$$

The values of the e.m.f. of Equations 24 and 25 are +1.68 and +1.59 V, respectively. The energy loss at 0.05 A cm^{-2} is greatger than 1.1 V at the fuel cell with Pd catalysts.

4. Conclusions

The activity of NO reduction in 1 M KOH increases in the order of the catalysts Pd ≥ Pt > Rh = Ir > Ru. The faradaic efficencies of N_2O formation decrease with decreasing NO flow rate and with the decrease in potential. The faradaic efficencies of N_2 formation increase with decreasing NO flow rate and with the decrease in potential. The reduction of NO to N_2 at 5 ml min^{-1} occurs selectively at potentials more negative than 0.1 V; the faradaic efficiency is approximately 95% at Pd catalysts.

Electricity generation and NO decomposition can be achieved simultaneously using the H_2–NO fuel cell reactor.

References

[1] D. Lorimer and A.T. Bell, *J. Catal.* **59** (1979) 223.
[2] M. L. Unland, *ibid.* **31** (1973) 159.
[3] H. Arai and H. Tominaga, *ibid.* **43** (1976) 131.
[4] R. Dictor, *ibid.* **109** (1988) 89.
[5] E. A. Hyde, R. Rudham and C. H. Rochester, *J. Chem., Faraday Trans.* **86** (1984) 531.
[6] K. Tomishige, K. Asakura and Y. Iwasawa, *J. Chem. Soc., Chem Commun.* (1993) 184.
[7] R. M. Lambert and C. M. Comrie, *Surf. Sci.* **46** (1974) 61.
[8] R. D. Ramsier, Q. Gao, H. N. Waltenburg and K. W. Lee, O. W. Nooij, L. Lefferts and J. T. Yates, Jr., *ibid.* **320** (1994) 209.
[9] T. W. Root, L. D. Schmidt and G. B. Fisher, *ibid.* **134** (1983) 30.
[10] L. J. J. Janssen, *Electrochim. Acta* **21** (1976) 811.
[11] M. J. Foral and S. H. Langer, *ibid.* **33** (1988) 257.
[12] D. Dutta and D. Landolt, *J. Electrochem. Soc.* **199** (1972) 1320.
[13] L. J. J. Janssen, M. M. J. Pieterse and E. Barendrecht, *Electrochim. Acta* **22** (1977) 27.
[14] D. L. Ehman and D. T. Sawyer, *J. Electroanal. Chem.* **16** (1974) 541.
[15] H. Ebert, R. Parsons, G. Ritzoulis and T. VanderNoot, *ibid.* **264** (1989) 181.
[16] K. E. Johnson and D. T. Sawyer, *ibid.* **49** (1974) 95.
[17] N. Furuya and H. Yoshiba, *ibid.* **303** (1989) 271.
[18] M. Shibata, K. Murase and N. Furuya, *Denki Kagaku*, **66** (1998) 811.
[19] N. Konishi, K. Hara, A. Kudo and T. Sakata, *Bull. Chem. Soc. Jpn.* **69** (1996) 2159.
[20] M. Watanabe, S. Motoo and N. Furuya, US Patent 4 931 168 (1990).